

Search for the $X(2370)$ and observation of $\eta_c \rightarrow \eta\eta\eta'$ in $J/\psi \rightarrow \gamma\eta\eta\eta'$

M. Ablikim,¹ M. N. Achasov,^{10,c} P. Adlarson,⁶⁴ S. Ahmed,¹⁵ M. Albrecht,⁴ R. Aliberti,²⁸ A. Amoroso,^{63a,63c} Q. An,^{60,47} X. H. Bai,⁵⁴ Y. Bai,⁴⁶ O. Bakina,²⁹ R. Baldini Ferroli,^{23a} I. Balossino,^{24a} Y. Ban,^{37,k} K. Begzsuren,²⁶ J. V. Bennett,⁵ N. Berger,²⁸ M. Bertani,^{23a} D. Bettoni,^{24a} F. Bianchi,^{63a,63c} J. Biernat,⁶⁴ J. Bloms,⁵⁷ A. Bortone,^{63a,63c} I. Boyko,²⁹ R. A. Briere,⁵ H. Cai,⁶⁵ X. Cai,^{1,47} A. Calcaterra,^{23a} G. F. Cao,^{1,51} N. Cao,^{1,51} S. A. Cetin,^{50a} J. F. Chang,^{1,47} W. L. Chang,^{1,51} G. Chelkov,^{29,b} D. Y. Chen,⁶ G. Chen,¹ H. S. Chen,^{1,51} M. L. Chen,^{1,47} S. J. Chen,³⁵ X. R. Chen,²⁵ Y. B. Chen,^{1,47} Z. J. Chen,^{20,l} W. S. Cheng,^{63c} G. Cibinetto,^{24a} F. Cossio,^{63c} X. F. Cui,³⁶ H. L. Dai,^{1,47} J. P. Dai,^{41,g} X. C. Dai,^{1,51} A. Dbeyssi,¹⁵ R. E. de Boer,⁴ D. Dedovich,²⁹ Z. Y. Deng,¹ A. Denig,²⁸ I. Denysenko,²⁹ M. Destefanis,^{63a,63c} F. De Mori,^{63a,63c} Y. Ding,³³ C. Dong,³⁶ J. Dong,^{1,47} L. Y. Dong,^{1,51} M. Y. Dong,^{1,47,51} S. X. Du,⁶⁸ J. Fang,^{1,47} S. S. Fang,^{1,51} Y. Fang,¹ R. Farinelli,^{24a} L. Fava,^{63b,63c} F. Feldbauer,⁴ G. Felici,^{23a} C. Q. Feng,^{60,47} M. Fritsch,⁴ C. D. Fu,¹ Y. Fu,¹ X. L. Gao,^{60,47} Y. Gao,^{37,k} Y. Gao,⁶¹ Y. Gao,^{60,47} Y. G. Gao,⁶ I. Garzia,^{24a,24b} E. M. Gersabeck,⁵⁵ A. Gilman,⁵⁶ K. Goetzen,¹¹ L. Gong,³³ W. X. Gong,^{1,47} W. Gradl,²⁸ M. Greco,^{63a,63c} L. M. Gu,³⁵ M. H. Gu,^{1,47} S. Gu,² Y. T. Gu,¹³ C. Y. Guan,^{1,51} A. Q. Guo,²² L. B. Guo,³⁴ R. P. Guo,³⁹ Y. P. Guo,^{9,h} A. Guskov,²⁹ S. Han,⁶⁵ T. T. Han,⁴⁰ T. Z. Han,^{9,h} X. Q. Hao,¹⁶ F. A. Harris,⁵³ N. Hüsken,⁵⁷ K. L. He,^{1,51} F. H. Heinsius,⁴ C. H. Heinz,²⁸ T. Held,⁴ Y. K. Heng,^{1,47,51} M. Himmelreich,^{11,f} T. Holtmann,⁴ Y. R. Hou,⁵¹ Z. L. Hou,¹ H. M. Hu,^{1,51} J. F. Hu,^{41,g} T. Hu,^{1,47,51} Y. Hu,¹ G. S. Huang,^{60,47} L. Q. Huang,⁶¹ X. T. Huang,⁴⁰ Y. P. Huang,¹ Z. Huang,^{37,k} T. Hussain,⁶² W. Ikegami Andersson,⁶⁴ W. Imoehl,²² M. Irshad,^{60,47} S. Jaeger,⁴ S. Janchiv,^{26,j} Q. Ji,¹ Q. P. Ji,¹⁶ X. B. Ji,^{1,51} X. L. Ji,^{1,47} H. B. Jiang,⁴⁰ X. S. Jiang,^{1,47,51} J. B. Jiao,⁴⁰ Z. Jiao,¹⁸ S. Jin,³⁵ Y. Jin,⁵⁴ T. Johansson,⁶⁴ N. Kalantar-Nayestanaki,⁵² X. S. Kang,³³ R. Kappert,⁵² M. Kavatsyuk,⁵² B. C. Ke,^{42,l} I. K. Keshk,⁴ A. Khoukaz,⁵⁷ P. Kiese,²⁸ R. Kiuchi,¹ R. Kliemt,¹¹ L. Koch,³⁰ O. B. Kolcu,^{50a,c} B. Kopf,⁴ M. Kuemmel,⁴ M. Kuessner,⁴ A. Kupsc,⁶⁴ M. G. Kurth,^{1,51} W. Kühn,³⁰ J. J. Lane,⁵⁵ J. S. Lange,³⁰ P. Larin,¹⁵ A. Lavania,²¹ L. Lavezzi,^{63a,63c} H. Leithoff,²⁸ M. Lellmann,²⁸ T. Lenz,²⁸ C. Li,³⁸ C. H. Li,³² Cheng Li,^{60,47} D. M. Li,⁶⁸ F. Li,^{1,47} G. Li,¹ H. Li,⁴² H. Li,^{60,47} H. B. Li,^{1,51} H. J. Li,^{9,h} J. L. Li,⁴⁰ J. Q. Li,⁴ Ke Li,¹ L. K. Li,¹ Lei Li,³ P. L. Li,^{60,47} P. R. Li,³¹ S. Y. Li,⁴⁹ W. D. Li,^{1,51} W. G. Li,¹ X. H. Li,^{60,47} X. L. Li,⁴⁰ Z. Y. Li,⁴⁸ H. Liang,^{60,47} H. Liang,^{1,51} Y. F. Liang,⁴⁴ Y. T. Liang,²⁵ G. R. Liao,¹² L. Z. Liao,^{1,51} J. Libby,²¹ C. X. Lin,⁴⁸ B. Liu,^{41,g} B. J. Liu,¹ C. X. Liu,¹ D. Liu,^{60,47} D. Y. Liu,^{41,g} F. H. Liu,⁴³ Fang Liu,¹ Feng Liu,⁶ H. B. Liu,¹³ H. M. Liu,^{1,51} Huanhuan Liu,¹ Huihui Liu,¹⁷ J. B. Liu,^{60,47} J. Y. Liu,^{1,51} K. Liu,¹ K. Y. Liu,³³ Ke Liu,⁶ L. Liu,^{60,47} Q. Liu,⁵¹ S. B. Liu,^{60,47} Shuai Liu,⁴⁵ T. Liu,^{1,51} W. M. Liu,^{60,47} X. Liu,³¹ Y. B. Liu,³⁶ Z. A. Liu,^{1,47,51} Z. Q. Liu,⁴⁰ Y. F. Long,^{37,k} X. C. Lou,^{1,47,51} F. X. Lu,¹⁶ H. J. Lu,¹⁸ J. D. Lu,^{1,51} J. G. Lu,^{1,47} X. L. Lu,¹ Y. Lu,¹ Y. P. Lu,^{1,47} C. L. Luo,³⁴ M. X. Luo,⁶⁷ P. W. Luo,⁴⁸ T. Luo,^{9,h} X. L. Luo,^{1,47} S. Lusso,^{63c} X. R. Lyu,⁵¹ F. C. Ma,³³ H. L. Ma,¹ L. L. Ma,⁴⁰ M. M. Ma,^{1,51} Q. M. Ma,¹ R. Q. Ma,^{1,51} R. T. Ma,⁵¹ X. N. Ma,³⁶ X. X. Ma,^{1,51} X. Y. Ma,^{1,47} Y. M. Ma,⁴⁰ F. E. Maas,¹⁵ M. Maggiora,^{63a,63c} S. Maldaner,⁴ S. Malde,⁵⁸ Q. A. Malik,⁶² A. Mangoni,^{23b} Y. J. Mao,^{37,k} Z. P. Mao,¹ S. Marcello,^{63a,63c} Z. X. Meng,⁵⁴ J. G. Messchendorp,⁵² G. Mezzadri,^{24a} T. J. Min,³⁵ R. E. Mitchell,²² X. H. Mo,^{1,47,51} Y. J. Mo,⁶ N. Yu. Muchnoi,^{10,c} H. Muramatsu,⁵⁶ S. Nakhoul,^{11,f} Y. Nefedov,²⁹ F. Nerling,^{11,f} I. B. Nikolaev,^{10,c} Z. Ning,^{1,47} S. Nisar,^{8,i} S. L. Olsen,⁵¹ Q. Ouyang,^{1,47,51} S. Pacetti,^{23b,23c} X. Pan,^{9,h} Y. Pan,⁵⁵ A. Pathak,¹ P. Patteri,^{23a} M. Pelizaeus,⁴ H. P. Peng,^{60,47} K. Peters,^{11,f} J. Pettersson,⁶⁴ J. L. Ping,³⁴ R. G. Ping,^{1,51} A. Pitka,⁴ R. Poling,⁵⁶ V. Prasad,^{60,47} H. Qi,^{60,47} H. R. Qi,⁴⁹ M. Qi,³⁵ T. Y. Qi,⁹ T. Y. Qi,² S. Qian,^{1,47} W. B. Qian,⁵¹ Z. Qian,⁴⁸ C. F. Qiao,⁵¹ L. Q. Qin,¹² X. S. Qin,⁴ Z. H. Qin,^{1,47} J. F. Qiu,¹ S. Q. Qu,³⁶ K. H. Rashid,⁶² K. Ravindran,²¹ C. F. Redmer,²⁸ A. Rivetti,^{63c} V. Rodin,⁵² M. Rolo,^{63c} G. Rong,^{1,51} Ch. Rosner,¹⁵ M. Rump,⁵⁷ A. Sarantsev,^{29,d} Y. Schelhaas,²⁸ C. Schnier,⁴ K. Schoenning,⁶⁴ M. Scodreggio,^{24a,24b} D. C. Shan,⁴⁵ W. Shan,¹⁹ X. Y. Shan,^{60,47} M. Shao,^{60,47} C. P. Shen,⁹ P. X. Shen,³⁶ X. Y. Shen,^{1,51} H. C. Shi,^{60,47} R. S. Shi,^{1,51} X. Shi,^{1,47} X. D. Shi,^{60,47} J. J. Song,⁴⁰ Q. Q. Song,^{60,47} W. M. Song,^{27,l} Y. X. Song,^{37,k} S. Sosio,^{63a,63c} S. Spataro,^{63a,63c} F. F. Sui,⁴⁰ G. X. Sun,¹ J. F. Sun,¹⁶ L. Sun,⁶⁵ S. S. Sun,^{1,51} T. Sun,^{1,51} W. Y. Sun,³⁴ X. Sun,^{20,l} Y. J. Sun,^{60,47} Y. K. Sun,^{60,47} Y. Z. Sun,¹ Z. T. Sun,¹ Y. H. Tan,⁶⁵ Y. X. Tan,^{60,47} C. J. Tang,⁴⁴ G. Y. Tang,¹ J. Tang,⁴⁸ J. X. Tang,^{60,47} V. Thoren,⁶⁴ I. Uman,^{50b} B. Wang,¹ B. L. Wang,⁵¹ C. W. Wang,³⁵ D. Y. Wang,^{37,k} H. P. Wang,^{1,51} K. Wang,^{1,47} L. L. Wang,¹ M. Wang,⁴⁰ M. Z. Wang,^{37,k} Meng Wang,^{1,51} W. H. Wang,⁶⁵ W. P. Wang,^{60,47} X. Wang,^{37,k} X. F. Wang,³¹ X. L. Wang,^{9,h} Y. Wang,⁴⁸ Y. Wang,^{60,47} Y. D. Wang,¹⁵ Y. F. Wang,^{1,47,51} Y. Q. Wang,¹ Z. Wang,^{1,47} Z. Y. Wang,¹ Ziyi Wang,⁵¹ Zongyuan Wang,^{1,51} D. H. Wei,¹² P. Weidenkaff,²⁸ F. Weidner,⁵⁷ S. P. Wen,¹ D. J. White,⁵⁵ U. Wiedner,⁴ G. Wilkinson,⁵⁸ M. Wolke,⁶⁴ L. Wollenberg,⁴ J. F. Wu,^{1,51} L. H. Wu,¹ L. J. Wu,^{1,51} X. Wu,^{9,h} Z. Wu,^{1,47} L. Xia,^{60,47} H. Xiao,^{9,h} S. Y. Xiao,¹ Y. J. Xiao,^{1,51} Z. J. Xiao,³⁴ X. H. Xie,^{37,k} Y. G. Xie,^{1,47} Y. H. Xie,⁶ T. Y. Xing,^{1,51} X. A. Xiong,^{1,51} G. F. Xu,¹ J. J. Xu,³⁵ Q. J. Xu,¹⁴ W. Xu,^{1,51} X. P. Xu,⁴⁵ Y. C. Xu,⁵¹ F. Yan,^{9,h} L. Yan,^{63a,63c} L. Yan,^{9,h} W. B. Yan,^{60,47} W. C. Yan,⁶⁸ Xu Yan,⁴⁵ H. J. Yang,^{41,g} H. X. Yang,¹ L. Yang,⁶⁵ R. X. Yang,^{60,47} S. L. Yang,^{1,51} Y. H. Yang,³⁵ Y. X. Yang,¹² Yifan Yang,^{1,51} Zhi Yang,²⁵ M. Ye,^{1,47} M. H. Ye,⁷ J. H. Yin,¹ Z. Y. You,⁴⁸ B. X. Yu,^{1,47,51} C. X. Yu,³⁶ G. Yu,^{1,51} J. S. Yu,^{20,l} T. Yu,⁶¹ C. Z. Yuan,^{1,51} W. Yuan,^{63a,63c} X. Q. Yuan,^{37,k} Y. Yuan,¹ Z. Y. Yuan,⁴⁸ C. X. Yue,³² A. Yuncu,^{50a,a} A. A. Zafar,⁶² Y. Zeng,^{20,l} B. X. Zhang,¹ Guangyi Zhang,¹⁶ H. Zhang,⁶⁰ H. H. Zhang,⁴⁸ H. Y. Zhang,^{1,47} J. L. Zhang,⁶⁶ J. Q. Zhang,⁴ J. Q. Zhang,³⁴ J. W. Zhang,^{1,47,51} J. Y. Zhang,¹ J. Z. Zhang,^{1,51}

Jianyu Zhang,^{1,51} Jiawei Zhang,^{1,51} Lei Zhang,³⁵ S. Zhang,⁴⁸ S. F. Zhang,³⁵ T. J. Zhang,^{41,g} X. Y. Zhang,⁴⁰ Y. Zhang,⁵⁸
 Y. H. Zhang,^{1,47} Y. T. Zhang,^{60,47} Yan Zhang,^{60,47} Yao Zhang,¹ Yi Zhang,^{9,h} Z. H. Zhang,⁶ Z. Y. Zhang,⁶⁵ G. Zhao,¹
 J. Zhao,³² J. Y. Zhao,^{1,51} J. Z. Zhao,^{1,47} Lei Zhao,^{60,47} Ling Zhao,¹ M. G. Zhao,³⁶ Q. Zhao,¹ S. J. Zhao,⁶⁸ Y. B. Zhao,^{1,47}
 Y. X. Zhao,²⁵ Z. G. Zhao,^{60,47} A. Zhemchugov,^{29,b} B. Zheng,⁶¹ J. P. Zheng,^{1,47} Y. Zheng,^{37,k} Y. H. Zheng,⁵¹ B. Zhong,³⁴
 C. Zhong,⁶¹ L. P. Zhou,^{1,51} Q. Zhou,^{1,51} X. Zhou,⁶⁵ X. K. Zhou,⁵¹ X. R. Zhou,^{60,47} A. N. Zhu,^{1,51} J. Zhu,³⁶ K. Zhu,¹
 K. J. Zhu,^{1,47,51} S. H. Zhu,⁵⁹ W. J. Zhu,³⁶ Y. C. Zhu,^{60,47} Z. A. Zhu,^{1,51} B. S. Zou,¹ and J. H. Zou¹

(BESIII Collaboration)

¹*Institute of High Energy Physics, Beijing 100049, People's Republic of China*

²*Beihang University, Beijing 100191, People's Republic of China*

³*Beijing Institute of Petrochemical Technology, Beijing 102617, People's Republic of China*

⁴*Bochum Ruhr-University, D-44780 Bochum, Germany*

⁵*Carnegie Mellon University, Pittsburgh, Pennsylvania 15213, USA*

⁶*Central China Normal University, Wuhan 430079, People's Republic of China*

⁷*China Center of Advanced Science and Technology, Beijing 100190, People's Republic of China*

⁸*COMSATS University Islamabad, Lahore Campus, Defence Road, Off Raiwind Road,
54000 Lahore, Pakistan*

⁹*Fudan University, Shanghai 200443, People's Republic of China*

¹⁰*G.I. Budker Institute of Nuclear Physics SB RAS (BINP), Novosibirsk 630090, Russia*

¹¹*GSI Helmholtzcentre for Heavy Ion Research GmbH, D-64291 Darmstadt, Germany*

¹²*Guangxi Normal University, Guilin 541004, People's Republic of China*

¹³*Guangxi University, Nanning 530004, People's Republic of China*

¹⁴*Hangzhou Normal University, Hangzhou 310036, People's Republic of China*

¹⁵*Helmholtz Institute Mainz, Johann-Joachim-Becher-Weg 45, D-55099 Mainz, Germany*

¹⁶*Henan Normal University, Xinxiang 453007, People's Republic of China*

¹⁷*Henan University of Science and Technology, Luoyang 471003, People's Republic of China*

¹⁸*Huangshan College, Huangshan 245000, People's Republic of China*

¹⁹*Hunan Normal University, Changsha 410081, People's Republic of China*

²⁰*Hunan University, Changsha 410082, People's Republic of China*

²¹*Indian Institute of Technology Madras, Chennai 600036, India*

²²*Indiana University, Bloomington, Indiana 47405, USA*

^{23a}*INFN Laboratori Nazionali di Frascati, I-00044 Frascati, Italy;*

^{23b}*INFN Sezione di Perugia, I-06100 Perugia, Italy;*

^{23c}*University of Perugia, I-06100 Perugia, Italy*

^{24a}*INFN Sezione di Ferrara, I-44122 Ferrara, Italy;*

^{24b}*University of Ferrara, I-44122 Ferrara, Italy*

²⁵*Institute of Modern Physics, Lanzhou 730000, People's Republic of China*

²⁶*Institute of Physics and Technology, Peace Avenue 54B, Ulaanbaatar 13330, Mongolia*

²⁷*Jilin University, Changchun 130012, People's Republic of China*

²⁸*Johannes Gutenberg University of Mainz, Johann-Joachim-Becher-Weg 45, D-55099 Mainz, Germany*

²⁹*Joint Institute for Nuclear Research, 141980 Dubna, Moscow region, Russia*

³⁰*Justus-Liebig-Universitaet Giessen, II. Physikalisches Institut, Heinrich-Buff-Ring 16,
D-35392 Giessen, Germany*

³¹*Lanzhou University, Lanzhou 730000, People's Republic of China*

³²*Liaoning Normal University, Dalian 116029, People's Republic of China*

³³*Liaoning University, Shenyang 110036, People's Republic of China*

³⁴*Nanjing Normal University, Nanjing 210023, People's Republic of China*

³⁵*Nanjing University, Nanjing 210093, People's Republic of China*

³⁶*Nankai University, Tianjin 300071, People's Republic of China*

³⁷*Peking University, Beijing 100871, People's Republic of China*

³⁸*Qufu Normal University, Qufu 273165, People's Republic of China*

³⁹*Shandong Normal University, Jinan 250014, People's Republic of China*

⁴⁰*Shandong University, Jinan 250100, People's Republic of China*

⁴¹*Shanghai Jiao Tong University, Shanghai 200240, People's Republic of China*

⁴²*Shanxi Normal University, Linfen 041004, People's Republic of China*

⁴³*Shanxi University, Taiyuan 030006, People's Republic of China*

- ⁴⁴Sichuan University, Chengdu 610064, People's Republic of China
⁴⁵Soochow University, Suzhou 215006, People's Republic of China
⁴⁶Southeast University, Nanjing 211100, People's Republic of China
⁴⁷State Key Laboratory of Particle Detection and Electronics, Beijing 100049, Hefei 230026, People's Republic of China
⁴⁸Sun Yat-Sen University, Guangzhou 510275, People's Republic of China
⁴⁹Tsinghua University, Beijing 100084, People's Republic of China
^{50a}Turkish Accelerator Center Particle Factory Group, Istanbul Bilgi University, 34060 Eyup, Istanbul, Turkey;
^{50b}Near East University, Nicosia, North Cyprus, 99138 Mersin 10, Turkey
⁵¹University of Chinese Academy of Sciences, Beijing 100049, People's Republic of China
⁵²University of Groningen, NL-9747 AA Groningen, The Netherlands
⁵³University of Hawaii, Honolulu, Hawaii 96822, USA
⁵⁴University of Jinan, Jinan 250022, People's Republic of China
⁵⁵University of Manchester, Oxford Road, Manchester M13 9PL, United Kingdom
⁵⁶University of Minnesota, Minneapolis, Minnesota 55455, USA
⁵⁷University of Muenster, Wilhelm-Klemm-Street 9, 48149 Muenster, Germany
⁵⁸University of Oxford, Keble Road, Oxford OX13RH, United Kingdom
⁵⁹University of Science and Technology Liaoning, Anshan 114051, People's Republic of China
⁶⁰University of Science and Technology of China, Hefei 230026, People's Republic of China
⁶¹University of South China, Hengyang 421001, People's Republic of China
⁶²University of the Punjab, Lahore 54590, Pakistan
^{63a}University of Turin and INFN, University of Turin, I-10125 Turin, Italy;
^{63b}University of Eastern Piedmont, I-15121 Alessandria, Italy;
^{63c}INFN, I-10125 Turin, Italy
⁶⁴Uppsala University, Box 516, SE-75120 Uppsala, Sweden
⁶⁵Wuhan University, Wuhan 430072, People's Republic of China
⁶⁶Xinyang Normal University, Xinyang 464000, People's Republic of China
⁶⁷Zhejiang University, Hangzhou 310027, People's Republic of China
⁶⁸Zhengzhou University, Zhengzhou 450001, People's Republic of China



(Received 13 December 2020; accepted 11 January 2021; published 29 January 2021)

Using a sample of 1.31×10^9 J/ψ events collected with the BESIII detector, we perform a study of $J/\psi \rightarrow \gamma\eta\eta\eta'$ to search for the $X(2370)$ and η_c in the $\eta\eta\eta'$ invariant mass distribution. No significant signal for the $X(2370)$ is observed, and we set an upper limit for the product branching fraction of $\mathcal{B}(J/\psi \rightarrow \gamma X(2370)) \cdot \mathcal{B}(X(2370) \rightarrow \eta\eta\eta') < 9.2 \times 10^{-6}$ at the 90% confidence level. A clear η_c signal is observed for the first time, yielding a product branching fraction of $\mathcal{B}(J/\psi \rightarrow \gamma\eta_c) \cdot \mathcal{B}(\eta_c \rightarrow \eta\eta\eta') = (4.86 \pm 0.62(\text{stat}) \pm 0.45(\text{sys})) \times 10^{-5}$.

DOI: 10.1103/PhysRevD.103.012009

^aAlso at Bogazici University, 34342 Istanbul, Turkey.

^bAlso at the Moscow Institute of Physics and Technology, Moscow 141700, Russia.

^cAlso at the Novosibirsk State University, Novosibirsk 630090, Russia.

^dAlso at the NRC "Kurchatov Institute," PNPI, 188300 Gatchina, Russia.

^eAlso at Istanbul Arel University, 34295 Istanbul, Turkey.

^fAlso at Goethe University Frankfurt, 60323 Frankfurt am Main, Germany.

^gAlso at Key Laboratory for Particle Physics, Astrophysics and Cosmology, Ministry of Education; Shanghai Key Laboratory for Particle Physics and Cosmology; Institute of Nuclear and Particle Physics, Shanghai 200240, People's Republic of China.

^hAlso at Key Laboratory of Nuclear Physics and Ion-beam Application (MOE) and Institute of Modern Physics, Fudan University, Shanghai 200443, People's Republic of China.

ⁱAlso at Harvard University, Department of Physics, Cambridge, Massachusetts 02138, USA.

^jPresent address: Institute of Physics and Technology, Peace Ave. 54B, Ulaanbaatar 13330, Mongolia.

^kAlso at State Key Laboratory of Nuclear Physics and Technology, Peking University, Beijing 100871, People's Republic of China.

^lAlso at School of Physics and Electronics, Hunan University, Changsha 410082, China.

I. INTRODUCTION

The non-Abelian property of quantum chromodynamics (QCD) permits the existence of glueballs formed by gluons, the gauge bosons of the strong force [1–3]. The search for glueballs is an important field of research in hadron physics. However, the identification of glueballs is difficult in both experiment and theory due to the possible mixing of the pure glueball states with nearby $q\bar{q}$ nonet mesons. Lattice QCD (in the quenched approximation) predicts the lowest-lying glueballs are scalar (mass 1.5–1.7 GeV/ c^2), tensor (mass 2.3–2.4 GeV/ c^2), and pseudoscalar (mass 2.3–2.6 GeV/ c^2) [4–8].

The radiative decay $J/\psi \rightarrow \gamma gg$ is a gluon-rich process and is therefore regarded as one of the most promising hunting grounds for glueballs [9,10]. A possible pseudoscalar glueball candidate, the $X(2370)$, is observed in the $\pi^+\pi^-\eta'$ invariant mass distribution through the decays of $J/\psi \rightarrow \gamma\pi^+\pi^-\eta'$ [11] and in the $K\bar{K}\eta'$ invariant mass distribution in the decays of $J/\psi \rightarrow \gamma K\bar{K}\eta'$ [12] with statistical significances of 6.4σ and 8.3σ , respectively. The measured mass is consistent with the LQCD prediction for the pseudoscalar glueball [6]. In a calculation using an effective Lagrangian that couples the pseudoscalar glueball to scalar and pseudoscalar mesons, the ratios of the branching fractions of the pseudoscalar glueball decays $\Gamma_{G \rightarrow \eta\eta'}/\Gamma_G^{\text{tot}}$, $\Gamma_{G \rightarrow K\bar{K}\eta'}/\Gamma_G^{\text{tot}}$, and $\Gamma_{G \rightarrow \pi\pi\eta'}/\Gamma_G^{\text{tot}}$ are predicted to be 0.00082, 0.011, and 0.090 [13], respectively, for an assumed glueball mass of 2.370 GeV/ c^2 . An observation of the $X(2370)$ in $J/\psi \rightarrow \gamma\eta\eta'$ would contribute to our understanding of this state. In parallel, we search for the η_c since this charmonium state has never been observed decaying to $\eta\eta\eta'$ [14].

In this paper, the $X(2370)$ and η_c are studied via $J/\psi \rightarrow \gamma\eta\eta\eta'$ using $(1310.6 \pm 7.0) \times 10^6$ J/ψ decays [15] collected with the BESIII detector in 2009 and 2012. The η' is reconstructed via the decay channels $\eta' \rightarrow \gamma\pi^+\pi^-$ and $\eta' \rightarrow \pi^+\pi^-\eta$, and η via the decay channel $\gamma\gamma$.

II. DETECTOR AND MONTE CARLO SIMULATIONS

The BESIII detector is a magnetic spectrometer [16] located at the Beijing Electron Positron Collider (BEPCII) [17]. The cylindrical core of the BESIII detector consists of a helium-based multilayer drift chamber (MDC), a plastic scintillator time-of-flight system (TOF), and a CsI(Tl) electromagnetic calorimeter (EMC), which are all enclosed in a superconducting solenoidal magnet providing a 1.0 T (0.9 T in 2012) magnetic field. The solenoid is supported by an octagonal flux-return yoke with resistive plate counter muon identifier modules interleaved with steel. The acceptance of charged particles and photons is 93% over the 4π solid angle. The charged-particle momentum resolution at 1 GeV/ c is 0.5% and the dE/dx resolution is 6% for the electrons from Bhabha scattering. The EMC

measures photon energies with a resolution of 2.5% (5%) at 1 GeV in the barrel (end cap) region. The time resolution of the TOF barrel part is 68 ps, while that of the end cap part is 110 ps.

Simulated samples produced with the GEANT4-based [18] Monte Carlo (MC) package, which includes the geometric description of the BESIII detector and the detector response, are used to determine the detection efficiency and to estimate the backgrounds. The simulation includes the beam energy spread and initial state radiation in the e^+e^- annihilations modeled with the generator KKMC [19]. The inclusive MC sample includes production of the J/ψ resonance as well as continuum processes incorporated with KKMC [19]. The known decay modes are modeled with EVTGen [20] using branching fractions taken from the Particle Data Group (PDG) [14], and the remaining unknown decays from the charmonium states with LundCharm [21]. Final state radiation from charged final state particles is incorporated with the PHOTOS package [22]. To estimate the selection efficiency and to optimize the selection criteria, signal MC events are generated for $J/\psi \rightarrow \gamma X(2370)$, $\gamma\eta_c \rightarrow \gamma\eta\eta\eta'$. The polar angle of the photon in the J/ψ center of mass system, θ_γ , follows a $1 + \cos^2\theta_\gamma$ distribution. The decay of $X(2370)/\eta_c \rightarrow \eta\eta\eta'$ is simulated using phase-space (PHSP) generator. So does the process $\eta' \rightarrow \eta\pi^+\pi^-$. To obtain the efficiency curves, MC events are generated for $J/\psi \rightarrow \gamma X$, $X \rightarrow \eta\eta\eta'$, where X means 0^{-+} non-resonant state. For the process $\eta' \rightarrow \gamma\pi^+\pi^-$, a generator taking into account both the $\rho - \omega$ interference and the box anomaly is used [23]. The analysis is performed in the framework of the BESIII offline software system [24] incorporating the detector calibration, event reconstruction, and data storage.

III. EVENT SELECTION

Charged tracks in the polar angle range $|\cos\theta| < 0.93$ are reconstructed from hits in the MDC. Tracks must extrapolate to within 10 cm of the interaction point in the beam direction and 1 cm in the plane perpendicular to the beam. Each track is assumed to be a pion and no particle identification is applied. Candidate events are required to have two charged tracks and zero net charge.

Photon candidates are required to have an energy deposition above 25 MeV in the barrel region ($|\cos\theta| < 0.80$) and 50 MeV in the end cap ($0.86 < |\cos\theta| < 0.92$). To exclude showers from charged tracks, the angle between the shower position and the charged tracks extrapolated to the EMC must be greater than 10° . A timing requirement in the EMC is used to suppress electronic noise and energy deposits unrelated to the event. At least six (seven) photons are required for the $\eta' \rightarrow \gamma\pi^+\pi^-$ ($\eta' \rightarrow \pi^+\pi^-\eta$) mode.

For the $J/\psi \rightarrow \gamma\eta\eta\eta'$, $\eta' \rightarrow \gamma\pi^+\pi^-$ channel, a six-constraint (6C) kinematic fit is performed to the hypothesis of $J/\psi \rightarrow \gamma\eta\eta\eta\pi^+\pi^-$. This includes a 4C fit to the J/ψ initial four-momentum and 1C fit of each pair of photons to have

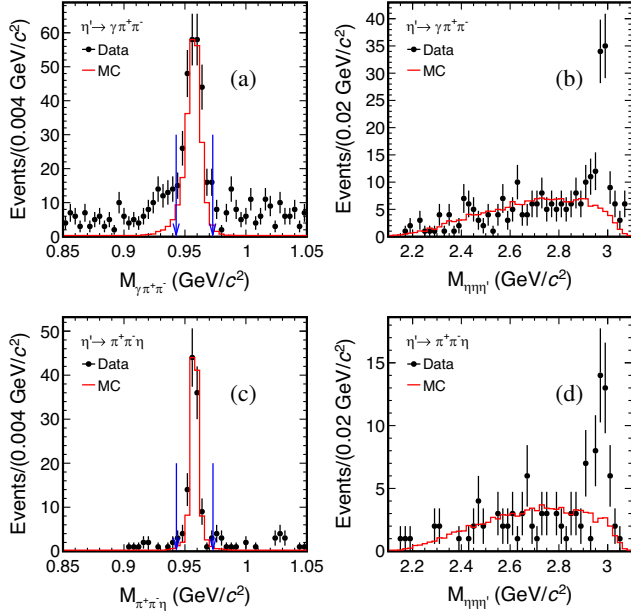


FIG. 1. Invariant mass distributions for the selected candidates of $J/\psi \rightarrow \gamma\eta\eta'$. Plots (a) and (b) are the invariant mass distributions of $\gamma\pi^+\pi^-$ and $\eta\eta'$ for $\eta' \rightarrow \gamma\pi^+\pi^-$, respectively. (c) and (d) are the invariant mass distributions of $\pi^+\pi^-\eta$ and $\eta\eta'$ for $\eta' \rightarrow \pi^+\pi^-\eta$, respectively. The dots with error bars are data and the histograms are for the signal MC samples (arbitrary normalization).

an invariant mass equal to that of an η . For events with more than six photon candidates, the combination with the minimum χ_{6C}^2 is selected, and $\chi_{6C}^2 < 30$ is required. Events with $|M_{\gamma\gamma} - m_{\pi^0}| < 0.02 \text{ GeV}/c^2$ are rejected to suppress background containing a π^0 , where the m_{π^0} is the nominal mass of the π^0 [14]. In order to reduce the background due to misreconstruction of the event, events with $|M_{\bar{\gamma}\bar{\gamma}} - m_{\eta}| < 0.02 \text{ GeV}/c^2$ are rejected, where the $M_{\bar{\gamma}\bar{\gamma}}$ is the invariant mass of all photon pairs except the pairs from the constrained η candidates and m_{η} is the nominal mass of η [14]. A clear η' signal is observed in the invariant mass distribution of $\gamma\pi^+\pi^-$ ($M_{\gamma\pi^+\pi^-}$), as shown in Fig. 1(a). The $\pi^+\pi^-$ invariant mass is required to be near the ρ mass region, $M_{\pi^+\pi^-} > 0.5 \text{ GeV}/c^2$. Candidate η' is reconstructed from the $\gamma\pi^+\pi^-$ pair with $|M_{\gamma\pi^+\pi^-} - m_{\eta'}| < 0.015 \text{ GeV}/c^2$, where the $m_{\eta'}$ is the nominal mass of the η' [14]. If there is more than one combination, we select the one with $M_{\gamma\pi^+\pi^-}$ closest to $m_{\eta'}$.

After applying the requirements above, we obtain the invariant mass distribution of $\eta\eta'$ ($M_{\eta\eta'}$), in which clear η_c signal is observed, as shown in Fig. 1(b).

For the $J/\psi \rightarrow \gamma\eta\eta'$, $\eta' \rightarrow \pi^+\pi^-\eta$ channel, a seven-constraint (7C) kinematic fit is performed to the hypothesis of $J/\psi \rightarrow \gamma\eta\eta\pi^+\pi^-$ in order to improve the η' mass resolution. If there are more than seven photon candidates, the combination with the minimum χ_{7C}^2 is retained, and

$\chi_{7C}^2 < 50$ is required. To suppress background from $\pi^0 \rightarrow \gamma\gamma$, $|M_{\gamma\gamma} - m_{\pi^0}| > 0.02 \text{ GeV}/c^2$ is required for all photon pairs. In order to reduce the background due to wrong reconstruction of the event, events with $|M_{\gamma_r\gamma_\eta} - m_{\eta}| < 0.02 \text{ GeV}/c^2$ are rejected, where the $M_{\gamma_r\gamma_\eta}$ is the invariant mass of the radiative photon (γ_r) directly from J/ψ decays paired with any photon from an η candidate decay (γ_η). The η' candidates are formed from $\pi^+\pi^-\eta$ combination satisfying $|M_{\pi^+\pi^-\eta} - m_{\eta'}| < 0.015 \text{ GeV}/c^2$ and the combination with $M_{\pi^+\pi^-\eta}$ closest to $m_{\eta'}$ is selected, where $M_{\pi^+\pi^-\eta}$ is the invariant mass of $\pi^+\pi^-\eta$, as shown in Fig. 1(c). Finally, the invariant mass distribution of $\eta\eta'$ ($M_{\eta\eta'}$), with a clear signal of η_c , is shown in Fig. 1(d).

IV. SIGNAL EXTRACTION

Potential backgrounds are studied using an inclusive MC sample of $1.2 \times 10^9 J/\psi$ decays. No significant peaking background is observed in the invariant mass distribution of $\eta\eta'$. Non- η' processes are studied using the η' mass sidebands, which are $[0.890, 0.920]$ and $[0.995, 1.025] \text{ GeV}/c^2$. No clear peak is observed in $X(2370)$ and η_c mass region from sideband study.

Efficiency curves obtained from 0^{++} PHSP MC simulation are shown in Figs. 2(a) and 2(b). Using double Gaussian function to fit the invariant spectrum of $\eta\eta'$ from signal MC samples generated with a zero width resonance, the mass resolutions of the $X(2370)$ in these two η' decay modes are determined to be $8.2 \text{ MeV}/c^2$ ($\eta' \rightarrow \gamma\pi^+\pi^-$) and $8.7 \text{ MeV}/c^2$ ($\eta' \rightarrow \pi^+\pi^-\eta$), while the mass resolutions of the η_c are determined to be $5.4 \text{ MeV}/c^2$ ($\eta' \rightarrow \gamma\pi^+\pi^-$) and $5.7 \text{ MeV}/c^2$ ($\eta' \rightarrow \pi^+\pi^-\eta$).

There is no obvious signal for the $X(2370)$ in $\eta\eta'$ invariant mass distributions in Figs. 1(b) and 1(d). We perform a simultaneous unbinned maximum likelihood fit to the $\eta\eta'$ distributions in the range of $[2.1, 2.7] \text{ GeV}/c^2$. The results are shown in Figs. 2(c) and 2(d), where the signal size represents the upper limit fit result of the $X(2370)$ rather than the negligible central value from the actual fit. The $X(2370)$ signal peak is represented by an efficiency-weighted nonrelativistic Breit-Wigner (BW) function convolved with a double Gaussian function to account for the mass resolution. Due to low statistics, the mass and width of the BW function are fixed to previously published BESIII results [11] while the parameters of the double Gaussian function are fixed to the results obtained from the fit of signal MC samples generated with zero width of the $X(2370)$. Interference between the $X(2370)$ and other components is ignored. The non- η' background events are described using η' mass sidebands and the yields are fixed in the fit; the remaining background is described by a second order Chebychev polynomial function with free parameters. In the simultaneous fit, the signal ratio for the two η' decay modes is fixed with a factor calculated by

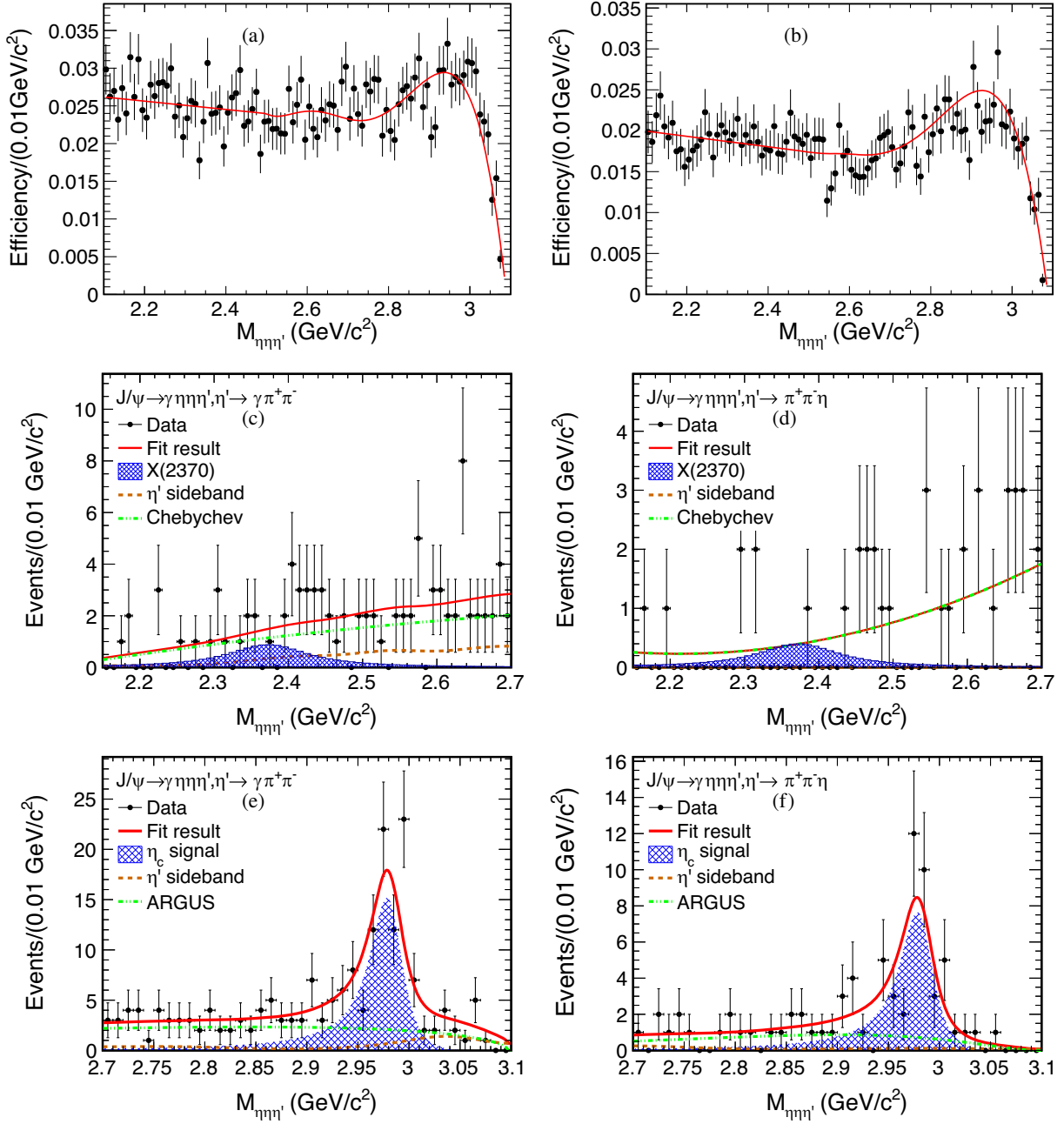


FIG. 2. Plots (a) and (b) are efficiency curves for the decays of $\eta' \rightarrow \gamma\pi^+\pi^-$ and $\eta' \rightarrow \pi^+\pi^-\eta$ obtained from $J/\psi \rightarrow \gamma X \rightarrow \gamma\eta\eta\eta'$ MC simulation, where X means 0^{-+} nonresonant state. Plots (c) and (d) are the simultaneous fit results for the X(2370) in the invariant mass distribution of $\eta\eta\eta'$ for the decays of $\eta' \rightarrow \gamma\pi^+\pi^-$ and $\eta' \rightarrow \pi^+\pi^-\eta$, respectively. Plots (e) and (f) are the fit results for η_c in the invariant mass distribution of $\eta\eta\eta'$ for the decays of $\eta' \rightarrow \gamma\pi^+\pi^-$ and $\eta' \rightarrow \pi^+\pi^-\eta$, respectively. The dots with error bars represent the data, the red solid curves show the fit results, the hatched areas represent the signal of the X(2370) scaled to the upper limit or the signal of the η_c , the brown dashed lines show the events from η' sideband, the green hyphenated lines represent the Chebychev polynomial function or the ARGUS function.

their branching fractions and efficiencies. Since no evident X(2370) signal is seen in $M_{\eta\eta\eta'}$, a Bayesian method is used to obtain the upper limit of the signal yield at the 90% confidence level (C.L.). To determine the upper limit of the signal yield, the distribution of normalized likelihood values for a series of expected signal event yields is taken as

the probability density function (PDF). The 90% C.L. yield, N^{UL} , is set such that 90% of the PDF area above zero yield is contained between 0 and N^{UL} . We repeat this procedure with different X(2370) signal shape parameters, fit ranges, η' sideband regions, and background shapes, and the maximum upper limit among these cases is selected.

TABLE I. Fit results of the signal yield for $J/\psi \rightarrow \gamma X(2370) \rightarrow \gamma\eta\eta\eta'$ and $J/\psi \rightarrow \gamma\eta_c \rightarrow \gamma\eta\eta\eta'$. The uncertainties are statistical only.

| Decay channel | $\eta' \rightarrow \gamma\pi^+\pi^-$ | $\eta' \rightarrow \pi^+\pi^-\eta$ |
|---|--------------------------------------|------------------------------------|
| $J/\psi \rightarrow \gamma X(2370) \rightarrow \gamma\eta\eta\eta'$ | < 15.2 | < 6.9 |
| $J/\psi \rightarrow \gamma\eta_c \rightarrow \gamma\eta\eta\eta'$ | 93.3 ± 11.9 | 43.2 ± 5.5 |

The obtained upper limits of the signal yields are listed in Table I. The MC detection efficiencies of $J/\psi \rightarrow \gamma X(2370) \rightarrow \gamma\eta\eta\eta'$ for the two η' decay modes are determined to be 2.95% ($\eta' \rightarrow \gamma\pi^+\pi^-$) and 2.32% ($\eta' \rightarrow \pi^+\pi^-\eta$). The upper limit of the product branching fraction is $\mathcal{B}(J/\psi \rightarrow \gamma X(2370)) \cdot \mathcal{B}(X(2370) \rightarrow \eta\eta\eta') < 8.70 \times 10^{-6}$.

A clear signal for the η_c is observed in $\eta\eta\eta'$ invariant mass distributions. We perform a simultaneous unbinned maximum likelihood fit to the $\eta\eta\eta'$ distributions in the range of [2.70, 3.10] GeV/ c^2 , as shown in Figs. 2(e) and 2(f). The η_c signal is described with an efficiency-weighted $E_\gamma^3 \times f_{\text{damp}}(E_\gamma) \times BW(m)$ function convolved with a double Gaussian function, where m is the $\eta\eta\eta'$ invariant mass and $E_\gamma = \frac{m_{J/\psi}^2 - m^2}{2m_{J/\psi}}$ is the energy of the transition photon in the rest frame of J/ψ . We also insert the function $f_{\text{damp}}(E_\gamma) = \frac{E_0^2}{E_0 E_\gamma + (E_0 - E_\gamma)^2}$ to damp the divergent tail at low mass arising from the E_γ^3 behavior, where $E_0 = \frac{m_{J/\psi}^2 - m_{\eta_c}^2}{2m_{J/\psi}}$ is the nominal energy of the transition photon [25]. The mass and width of the η_c are fixed to PDG values [14]. Interference between η_c and other components is ignored. Backgrounds are modeled with similar components as for the fit of the $X(2370)$ discussed above, while the Chebychev polynomial is replaced with an ARGUS function [26]. The obtained signal yields, which have correlated uncertainties due to the constrained fit, for $J/\psi \rightarrow \gamma\eta_c \rightarrow \gamma\eta\eta\eta'$ are listed in Table I. The detection efficiencies of $J/\psi \rightarrow \gamma\eta_c \rightarrow \gamma\eta\eta\eta'$ for two η' decay modes are determined to be 2.94% ($\eta' \rightarrow \gamma\pi^+\pi^-$) and 2.35% ($\eta' \rightarrow \pi^+\pi^-\eta$). We observe some disagreements in the data versus MC simulated $\eta\eta$, $\eta\eta'$, and $\eta\eta\eta'$ invariant mass spectra. We employ a machine learning (ML) method [27] to reweight the signal MC events based on the meson candidate's four-momenta. This reduces the inconsistency between data and signal MC, providing an accurate efficiency. The product branching fraction of $J/\psi \rightarrow \gamma\eta_c \rightarrow \gamma\eta\eta\eta'$ is then determined to be $(4.86 \pm 0.62(\text{stat})) \times 10^{-5}$. The statistical significance of η_c is determined to be 8.1σ .

V. SYSTEMATIC UNCERTAINTIES

Several sources of systematic uncertainties are considered, including the data-MC efficiency differences in the MDC tracking and the photon detection efficiency, the

kinematic fit, and the mass window requirements for the π^0 , η , ρ , and η' . Uncertainties associated with the fit ranges, the background shapes, the sideband regions, quantum number of $X(2370)$, the signal shape parameters of η_c , damping factor, efficiency calculation, intermediate resonance decay branching fractions, and the total number of J/ψ events are considered.

A. Efficiency estimation

The MDC tracking efficiencies of charged pions are investigated using a clean control sample of $J/\psi \rightarrow p\bar{p}\pi^+\pi^-$ [28]. The difference in tracking efficiencies between data and MC simulation is 1.0% for each charged pion. The photon detection efficiency is studied with a clean sample of $J/\psi \rightarrow \rho^0\pi^0$ [29]. The result shows that the data-MC efficiency difference is 1.0% per photon.

The systematic uncertainties associated with the kinematic fit are studied with the track helix parameter correction method, as described in Ref. [30]. The differences with respect to those without corrections are taken as the systematic uncertainties.

Due to the difference in the mass resolution between data and MC simulation, the uncertainties related to the $M_{\pi^+\pi^-}$ and η' mass window requirements are investigated by smearing the MC simulation to improve the consistency between data and MC simulation. The differences of the detection efficiency before and after smearing are assigned as systematic uncertainties for the $M_{\pi^+\pi^-}$ and η' mass window requirements. The uncertainties from the π^0 and η mass window requirements are estimated by varying those mass windows. The changes in the resultant branching fractions are assigned as the systematic uncertainties from these items.

To study uncertainties related to the efficiency calculation with the ML method, we generate a generic MC sample with $J/\psi \rightarrow \gamma\eta_c$, $\eta_c \rightarrow f_2(1810)\eta'$ ($f_2(1810) \rightarrow \eta\eta$) process to represent the signal and $J/\psi \rightarrow \gamma\eta\eta\eta'$ as the non- η_c background. The numbers of signal and background events are fixed to fitting results. The efficiency difference between the generic MC sample and the ML method is taken as systematic uncertainty from this item. Furthermore, we consider the effects arising from different quantum numbers of the $X(2370)$. We generate $J/\psi \rightarrow \gamma X(2370)$ decays under the assumption of a $\sin^2\theta_\gamma$ angular distribution. The resulting difference of efficiency with respect to the nominal value is taken as systematic uncertainty.

B. Fit to the signal

Systematic uncertainties related to the $X(2370)$ signal treatment are already accounted for in the upper limit yield, as discussed previously; here, we discuss the treatment of the η_c signal. To study the uncertainties from the fit range, the fits are repeated with different fit ranges, and the largest

difference among these signal yields is taken as systematic uncertainty. The uncertainties from the η' sideband region are estimated by using alternative sideband regions. The maximum difference among signal yields with respect to the nominal value is taken as the uncertainty. To estimate the uncertainty associated with the background shape, alternative fit with a truncated second order polynomial for the background is performed. The maximum difference in signal yields with respect to the nominal value is taken as systematic uncertainty. To study the uncertainty associated with the parameters of η_c , we change these values by $\pm 1\sigma$ and repeat the fit. The largest difference from our nominal result among these alternative fits is taken as the uncertainty. The uncertainty due to damping factor is estimated by using an alternative form of the damping factor, which was used by the CLEO Collaboration [31], $f_{\text{damp}}(E_\gamma) = \exp(-\frac{E_\gamma^2}{8\beta^2})$, where E_γ is the energy of the transition photon and $\beta = 0.065$ GeV. The difference between the results with different damping factor forms is taken as the systematic uncertainty.

C. Other uncertainties

The uncertainties on the intermediate decay branching fractions of $\eta' \rightarrow \gamma\pi^+\pi^-$, $\eta' \rightarrow \pi^+\pi^-\eta$, and $\eta \rightarrow \gamma\gamma$ are taken from the world average values [14], which are 1.7%, 1.6%, and 0.5%, respectively. The systematic uncertainty due to the number of J/ψ events is determined as 0.5% according to Ref. [15].

A summary of all the uncertainties is shown in Tables II and III. The total systematic uncertainties are obtained by adding all individual uncertainties in quadrature, assuming all sources to be independent.

In this paper, $J/\psi \rightarrow \gamma\eta\eta'$ is studied with two η' decay modes. The measurements from the two η' decay modes

TABLE II. Systematic uncertainties for determination of the upper limit of branching fraction of $J/\psi \rightarrow \gamma X(2370) \rightarrow \gamma\eta\eta'$ (in %). The items with * are common uncertainties of both η' decay modes.

| Source | $\eta' \rightarrow \gamma\pi^+\pi^-$ | $\eta' \rightarrow \pi^+\pi^-\eta$ |
|---|--------------------------------------|------------------------------------|
| MDC tracking* | 2.0 | 2.0 |
| Photon detection* | 6.0 | 7.0 |
| Kinematic fit | 1.0 | 1.0 |
| ρ mass window | 2.4 | ... |
| η' mass window | 1.2 | 0.6 |
| π^0 veto | 18.6 | 5.3 |
| η veto | 15.5 | 0.6 |
| Quantum numbers of $X(2370)$ | 13.4 | 10.5 |
| $B(\eta' \rightarrow \gamma\pi^+\pi^-)$ | 1.7 | ... |
| $B(\eta' \rightarrow \pi^+\pi^-\eta)$ | ... | 1.6 |
| $B(\eta \rightarrow \gamma\gamma)^*$ | 1.0 | 1.5 |
| Number of J/ψ events* | 0.5 | 0.5 |
| Total | 28.6 | 14.1 |

TABLE III. Systematic uncertainties for the determination of the branching fraction of $J/\psi \rightarrow \gamma\eta_c \rightarrow \gamma\eta\eta'$ (in %). The items with * are common uncertainties of both η' decay modes.

| Source | $\eta' \rightarrow \gamma\pi^+\pi^-$ | $\eta' \rightarrow \pi^+\pi^-\eta$ |
|---|--------------------------------------|------------------------------------|
| MDC tracking* | 2.0 | 2.0 |
| Photon detection* | 6.0 | 7.0 |
| Kinematic fit | 1.0 | 1.0 |
| ρ mass window | 1.6 | ... |
| η' mass window | 0.1 | 0.1 |
| π^0 veto | 0.6 | 1.5 |
| η veto | 1.2 | 0.0 |
| Efficiency calculation with ML | 1.4 | 1.4 |
| Fit range | 1.9 | 1.9 |
| Sideband region | 0.0 | 2.2 |
| Background shape | 11.7 | 5.9 |
| $B(\eta' \rightarrow \gamma\pi^+\pi^-)$ | 1.7 | ... |
| $B(\eta' \rightarrow \pi^+\pi^-\eta)$ | ... | 1.6 |
| $B(\eta \rightarrow \gamma\gamma)^*$ | 1.0 | 1.5 |
| Number of J/ψ events* | 0.5 | 0.5 |
| Parameters of η_c | 2.8 | 2.8 |
| Damping factor | 1.7 | 1.7 |
| Total | 14.2 | 10.8 |

are, therefore, combined by considering the difference of uncertainties for these two measurements. The combination of common and independent systematic uncertainties for the two η' decay modes is calculated with weighted least squares method [32]. The total systematic uncertainties are 12.8% and 9.2% for $\mathcal{B}(J/\psi \rightarrow \gamma X(2370)) \cdot \mathcal{B}(X(2370) \rightarrow \eta\eta')$ and $\mathcal{B}(J/\psi \rightarrow \gamma\eta_c) \cdot \mathcal{B}(\eta_c \rightarrow \eta\eta')$, respectively.

VI. RESULTS AND SUMMARY

Using a sample of 1.31×10^9 J/ψ events collected with the BESIII detector, the decays of $J/\psi \rightarrow \gamma\eta\eta'$ are investigated using the two η' decay modes, $\eta' \rightarrow \gamma\pi^+\pi^-$ and $\eta' \rightarrow \pi^+\pi^-\eta$, $\eta \rightarrow \gamma\gamma$.

No evident signal for the $X(2370)$ is observed in the $\eta\eta\eta'$ invariant mass distribution. To obtain the signal upper limit, we use the Bayesian method and perform unbinned maximum likelihood fits to the invariant mass spectrum of $\eta\eta\eta'$ with a series of expected signal yields. The distribution of normalized likelihood values is taken as the PDF for the expected signal yields. The final upper limit of the product branching fraction of $J/\psi \rightarrow \gamma X(2370) \rightarrow \eta\eta\eta'$ incorporates the 12.8% relative systematic uncertainty by convolving the likelihood distribution with a Gaussian function,

$$L(N') = \int_0^\infty L(N) \frac{1}{\sqrt{2\pi}\sigma_{\text{sys}}} \exp\left[-\frac{(N' - N)^2}{2\sigma_{\text{sys}}^2}\right] dN, \quad (1)$$

where $L(N)$ is the likelihood distribution, $\sigma_{\text{sys}} = 0.128N$, and N is the input signal yield. The resulting upper limit of $\mathcal{B}(J/\psi \rightarrow \gamma X(2370) \rightarrow \gamma\eta\eta')$ is estimated to be

9.2×10^{-6} , which is not in contradiction with the value predicted in Ref. [13] where $X(2370)$ is assumed as a pseudoscalar glueball. To understand the nature of $X(2370)$, it is mandatory to measure its spin and parity and to search for it in more decay modes with higher statistics.

A clear η_c signal is observed for the first time in the $\eta\eta\eta'$ invariant mass spectrum, the product branching fraction of $\mathcal{B}(J/\psi \rightarrow \gamma\eta_c) \cdot \mathcal{B}(\eta_c \rightarrow \eta\eta\eta')$ is determined to be $(4.86 \pm 0.62(\text{stat}) \pm 0.45(\text{sys})) \times 10^{-5}$, which is compatible with the theoretical prediction of partial decay width of $\eta_c \rightarrow \eta\eta\eta'$ in Ref. [33].

ACKNOWLEDGMENTS

The BESIII Collaboration thanks the staff of BEPCII and the IHEP computing center for their strong support. This work was supported in part by National Key Basic Research Program of China under Contract No. 2015CB856700; National Natural Science Foundation of China (NSFC) under Contracts No. 11625523, No. 11635010, No. 11675183, No. 11735014, No. 11822506, No. 11835012, No. 11922511, No. 11935015, No. 11935016,

No. 11935018, No. 11961141012 and No. 12061131003; the Chinese Academy of Sciences (CAS) Large-Scale Scientific Facility Program; Joint Large-Scale Scientific Facility Funds of the NSFC and CAS under Contracts No. U1732103, No. U1732263, and No. U1832207; CAS Key Research Program of Frontier Sciences under Contracts No. QYZDJ-SSW-SLH003 and No. QYZDJ-SSW-SLH040; 100 Talents Program of CAS; Institute of Nuclear and Particle Physics (INPAC) and Shanghai Key Laboratory for Particle Physics and Cosmology; ERC under Contract No. 758462; German Research Foundation DFG under Contract No. 443159800, Collaborative Research Center CRC 1044, FOR 2359, FOR 2359, GRK 214; Istituto Nazionale di Fisica Nucleare, Italy; Ministry of Development of Turkey under Contract No. DPT2006K-120470; National Science and Technology fund; Olle Engkvist Foundation under Contract No. 200-0605; STFC (United Kingdom); the Knut and Alice Wallenberg Foundation (Sweden) under Contract No. 2016.0157; The Royal Society, UK under Contracts No. DH140054 and No. DH160214; the Swedish Research Council; U.S. Department of Energy under Contracts No. DE-FG02-05ER41374 and No. DE-SC-0012069.

-
- [1] C. Amsler and N. A. Tornqvist, *Phys. Rep.* **389**, 61 (2004).
 - [2] E. Klempf and A. Zaitsev, *Phys. Rep.* **454**, 1 (2007).
 - [3] V. Crede and C. A. Meyer, *Prog. Part. Nucl. Phys.* **63**, 74 (2009).
 - [4] G. S. Bali *et al.* (UKQCD Collaboration), *Phys. Lett. B* **309**, 378 (1993).
 - [5] C. J. Morningstar and M. Peardon, *Phys. Rev. D* **60**, 034509 (1999).
 - [6] Y. Chen *et al.*, *Phys. Rev. D* **73**, 014516 (2006).
 - [7] E. Gregory, A. Irving, B. Lucini, C. McNeile, A. Rago, C. Richards, and E. Rinaldi, *J. High Energy Phys.* **10**(2012) 170.
 - [8] W. Sun, L.-C. Gui, Y. Chen, M. Gong, C. Liu, Y.-B. Liu, Z. Liu, J.-P. Ma, and J.-B. Zhang, *Chin. Phys. C* **42**, 093103 (2018).
 - [9] M. B. Cakir and G. R. Farrar, *Phys. Rev. D* **50**, 3268 (1994).
 - [10] F. E. Close, G. R. Farrar, and Z. P. Li, *Phys. Rev. D* **55**, 5749 (1997).
 - [11] M. Ablikim *et al.* (BESIII Collaboration), *Phys. Rev. Lett.* **106**, 072002 (2011).
 - [12] M. Ablikim *et al.* (BESIII Collaboration), *Eur. Phys. J. C* **80**, 746 (2020).
 - [13] W. I. Eshraim, S. Janowski, F. Giacosa, and D. H. Rischke, *Phys. Rev. D* **87**, 054036 (2013).
 - [14] P. A. Zyla *et al.* (Particle Data Group), *Prog. Theor. Exp. Phys.* (2020), 083C01.
 - [15] M. Ablikim *et al.* (BESIII Collaboration), *Chin. Phys. C* **41**, 013001 (2017).
 - [16] M. Ablikim *et al.* (BESIII Collaboration), *Nucl. Instrum. Methods Phys. Res., Sect. A* **614**, 345 (2010).
 - [17] C. H. Yu *et al.*, *Proceedings of IPAC2016, Busan, Korea* (2016), <https://doi.org/10.18429/JACoW-IPAC2016-TUYA01>.
 - [18] S. Agostinelli *et al.* (GEANT4 Collaboration), *Nucl. Instrum. Methods Phys. Res., Sect. A* **506**, 250 (2003).
 - [19] S. Jadach, B. F. L. Ward, and Z. Was, *Phys. Rev. D* **63**, 113009 (2001); *Comput. Phys. Commun.* **130**, 260 (2000).
 - [20] D. J. Lange, *Nucl. Instrum. Methods Phys. Res., Sect. A* **462**, 152 (2001); R. G. Ping, *Chin. Phys. C* **32**, 599 (2008).
 - [21] J. C. Chen, G. S. Huang, X. R. Qi, D. H. Zhang, and Y. S. Zhu, *Phys. Rev. D* **62**, 034003 (2000); R. L. Yang, R. G. Ping, and H. Chen, *Chin. Phys. Lett.* **31**, 061301 (2014).
 - [22] E. Richter-Was, *Phys. Lett. B* **303**, 163 (1993).
 - [23] M. Ablikim *et al.* (BESIII Collaboration), *Phys. Rev. Lett.* **120**, 242003 (2018).
 - [24] W. D. Li *et al.*, in *Proceeding of CHEP06, Mumbai, India, 2006*, edited by Sunanda Banerjee (Tata Institute of Fundamental Research, Mumbai, 2006).
 - [25] V. V. Anashin *et al.* (KEDR Collaboration), *Int. J. Mod. Phys. Conf. Ser.* **02**, 188 (2011).
 - [26] H. Albrecht *et al.* (ARGUS Collaboration), *Phys. Lett. B* **241**, 278 (1990).
 - [27] B. Liu, X. Xiong, G. Hou, S. Song, and L. Shen, *EPJ Web Conf.* **214**, 06033 (2019).

-
- [28] M. Ablikim *et al.* (BESIII Collaboration), *Phys. Rev. D* **85**, 092012 (2012).
- [29] M. Ablikim *et al.* (BESIII Collaboration), *Phys. Rev. D* **81**, 052005 (2010).
- [30] M. Ablikim *et al.* (BESIII Collaboration), *Phys. Rev. D* **87**, 012002 (2013).
- [31] R. E. Mitchell *et al.* (CLEO Collaboration), *Phys. Rev. Lett.* **102**, 011801 (2009).
- [32] G. D'Agostini, *Nucl. Instrum. Methods Phys. Res., Sect. A* **346**, 306 (1994).
- [33] W. I. Eshraim and C. S. Fischer, *Eur. Phys. J. A* **54**, 139 (2018).